Engineering Structures 32 (2010) 2166–2174

Contents lists available at ScienceDirect

Engineering Structures

journal homepage: www.elsevier.com/locate/engstruct

Non-stationary random vibration of bridges under vehicles with variable speed

Xinfeng Yin [a,c], Zhi Fang [a,*], C.S. Cai [b], Lu Deng [b]

[a] College of Civil Engineering, Hunan University, Changsha, 410082, China

[b] Department of Civil and Environmental Engineering, Louisiana State University, Baton Rouge, LA, 70803, USA

[c] School of Civil Engineering, Changsha University of Science and Technology, 45 Chiling Road, Tianxin Distr, Changsha, 410076, China

ARTICLE INFO

Article history:
Received 7 May 2009
Received in revised form
11 March 2010
Accepted 15 March 2010
Available online 22 April 2010

Keywords:
Vehicle
Bridge
Interaction
Variable speed
Non-stationary random process

ABSTRACT

Most researchers assumed the road surface inputs as stationary random process in time domain when studying vehicles with variable speed. This assumption was made to avoid the complexity of the non-stationary random processes. This paper presented a new method of analyzing the non-stationary random response of bridges. Using the covariance equivalence technique, the non-stationary random responses of wheels in time domain were obtained, and thus a new method of analyzing the non-stationary random response of bridges was developed. A two-axle vehicle model and three bridge models were analyzed, namely, a single-span uniform Bernoulli–Euler beam, a three-span stepped beam, and a three-span continuous non-uniform bridge deck. The bridge–vehicle coupling equations were established by combining the equations of motion of both the bridge and the vehicle using the displacement relationship and the interaction force relationship at the contact points. The numerical results indicated that the responses of the tires induced by the road roughness are the non-stationary process, and the amplitudes of responses change as the vehicle velocity varies. Using the responses of the tires as the inputs to study the non-stationary vibration of bridge–vehicle system with variable speed one can obtain more accurate solutions.

1. Introduction

The problem of interaction between vehicles and bridges has attracted much attention over the last few decades due to the drastic increase of the proportion of heavy and high-speed vehicles in highway and railway traffic. Many numerical methods were developed to study the influence of different factors on the dynamic behavior of bridges. Bridge structures were modeled with the finite element method using three-node Euler–Bernoulli beam elements [1–4], eight-node quadrilateral Kirchhoff plate/shell elements [5], and an assemblage of beam and plate elements [6]. Vehicles were modeled with different degrees of complexity. The simplest model was the quarter truck vehicle model [7,8]. Another two common models were the two-dimensional model [9] and the three-dimensional model [10–17]. Based on the models described above, the bridge–vehicle system was divided into subsystems with an interface between the bridge and the vehicle. The equations of motion of the bridge and the vehicle were in general solved separately by an iterative procedure [5]. A vehicle–bridge interaction element was developed and used to solve the problem with a series of vehicles moving in the same direction across a bridge [18,19].

When investigating the dynamic response for vehicles with variable speed, most of the previous studies either did not realize the non-stationary nature of the random response [20–23] or the non-stationary random response of the bridge–vehicle system was simplified as stationary response in time domain [24–28]. While this simplification avoids the complexity of the non-stationary random processes and significantly reduces the computation effort, verification of this simplification needs to be performed before using it with confidence.

In general, road roughness can be simulated as a stationary random process in space domain, while a vehicle moves with a constant speed. It is also a stationary random process in time domain, and this has been concluded by Honda et al. [29], Dodds and Robson [30], and Marcondes et al. [31]. Therefore, the response of the tire induced by the road roughness is a stationary random process in time domain. However, when a vehicle is traveling at variable speed, as will be shown later, the response of the tire induced by the road roughness is essentially a non-stationary random process in time domain [32–36]. As a result, the vibration responses of the vehicle–bridge system caused by road roughness should be considered as a non-stationary random vibration response. If the stationary random process is also used to simulate the road roughness, as in Refs. [24–26], this character of non-stationary vibration cannot be obtained. Therefore, introducing a new method to study this non-stationary

* Corresponding author. Tel.: +86 731 8821432; fax: +86 731 8821432.
E-mail addresses: ZACKFANG@163.com, fangzhi2000@sina.com (Z. Fang).

0141-0296/$ – see front matter © 2010 Elsevier Ltd. All rights reserved.
doi:10.1016/j.engstruct.2010.03.019

Nomenclature

x_i ($i = 1, 2, 3, 4, 5$)	Vertical displacements of the centroid of the vehicle
m_f, m_r, m_p, m_b	Mass of front the axle, rear axle, seat and tractor
J	Rotational moment of inertia of the tractor
$k_p, k_f, k_r, c_p, c_f, c_r$	Stiffness and damping of the each axles
k_{tf}, k_{tr}	Stiffness of the front and rear wheels
l_1, l_2, l_3	Distances from the front axle, rear axle, and the centroid of seat to the centroid of tractor
$q_f(t), q_r(t)$	Non-stationary random responses of the front and rear wheels
$m(x)$	Mass per unit length of the beam
$E(x), c$	Young's modulus and damping of the beam
$I(x)$	Moment of inertia for the cross-section of the beam
$y(x, t)$	Vertical displacement of the beam at position x and time t
$\dot{s}, \ddot{s}$	Velocity and acceleration of the vehicle
G_1, G_2	Vehicle gravity distributed to the front and rear axles
$\xi_i(t), \phi_i(x)$	The ith generalized modal coordinate and the ith mode shape of the beam ω_i natural frequencies of the beam
η_i	Percentage of the critical damping for the ith mode of the beam
M, C, K	Mass, damping, and stiffness matrices of the vehicle–bridge system
P, U	Global load vector and the global displacement vector of the entire system
$s_q(n)$	Spatial power spectral density
$s_q(n_0)$	Coefficient of road roughness
n	Spatial frequency (1/m)
Ω_q	Spatial angular frequency
Ω_c	Lowest cut-off angular frequency
$H(\Omega_q)$	The transfer function
S_W	The PSD of white noise
$W(s_c)$	Stationary white noise processes having a frequency modulated form
$q_f(s_c)$	Stationary random road surface inputs in space domain
$W_1(t)$	The stationary white noise process
$\delta(\cdot)$	The Dirac delta function
τ	Interval time between the front and rear wheels
I	Dynamic impact factor of the bridge
R_{dm}, R_{sm}	Maximum vertical dynamic and static deflections of the bridge under the vehicle loading
k	Elastomeric bearing calculated in the mode shape of the beam

vibration is significant. A few approaches of analyzing the non-stationary random vibration have been developed when the vehicle is subjected to acceleration or braking. The state-space approaches to analyze the non-stationary response of a vehicle traveling on a homogeneous rough road were presented [32,33]. In their study, the vehicle dynamics were modeled by liner ordinary differential equations in time domain while the excitation process of rough road was modeled by a differential equation in spatial domain. Nigam and Yaday [34] presented another method for solving non-stationary response of a vehicle, in which differential equations with variable coefficients were first established in space domain, and the time changing covariance was then computed. Based on this work, two different improved methods with higher computational efficiency were proposed by Hwang et al. [35], and Zhang et al. [36], respectively. Sasidhar and Talukdar [37] used the Monte Carlo simulation technique to simulate deck profile for generating input samples in numerical integration of the system equations. However, the computation effort of this method is very large.

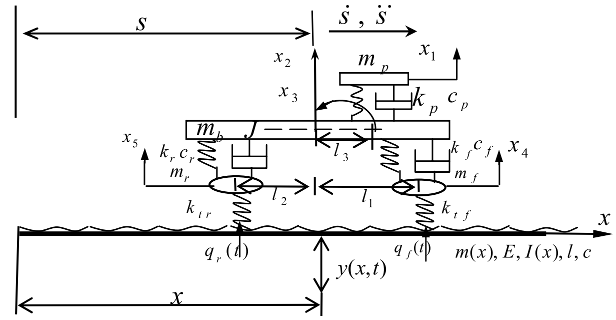

Fig. 1. Schematic of the bridge–vehicle coupled system.

This paper presented a new method of simulating the non-stationary random responses of the vehicle tires and thus developed a new method of analyzing the non-stationary random response of bridges. Using the covariance equivalence technique, the non-stationary random responses of the moving tires induced by the road roughness in time domain were obtained, and then this non-stationary response can be treated as the non-stationary inputs of the bridge–vehicle coupled system. A two-axle vehicle model and three bridge models were analyzed, namely, a single-span uniform Bernoulli–Euler beam, a three-span stepped beam, and a three-span continuous non-uniform bridge deck. The vehicle–bridge coupling equations were established by combining the equations of motion of both the bridge and vehicle using the displacement relationship and the interaction force relationship at the contact points. The differential equations of motion of the coupled systems were derived from the Lagrangian formulation. The stationary random process and the non-stationary response of tires are respectively treated as the inputs of the bridge–vehicle coupled system. The comparison of the effect of the two inputs on the mid-span deflection and the impact factors were compared with different parameters including the coefficient of surface roughness, vehicle acceleration, and vehicle braking.

2. Vehicle and bridge models

A vehicle model with five-degree-of-freedom (5-DOF) shown in Fig. 1 was used as a representative of modern freight vehicles. The five DOFs are denoted by x_i ($i = 1, 2, 3, 4, 5$). The masses of the front and rear axle assembly are denoted by m_f and m_r, and the masses of the seat and tractor are denoted as m_p and m_b, respectively. J represents the rotational moment of inertia of the tractor. Each vehicle axles has its stiffness and damping, they are denoted by k_p, k_f, and k_r, and c_p, c_f, and c_r, respectively. The stiffness of the front and rear wheels are denoted by k_{tf} and k_{tr}. l_1, l_2, and l_3 are distances from the front axle, rear axle, and the centroid of seat to the centroid of tractor, respectively. The non-stationary random responses induced by the road roughness of the front and rear wheels are denoted by $q_f(t)$ and $q_r(t)$, respectively.

The three bridge superstructures model used in the present study are: a single-span uniform Bernoulli–Euler beam, a three-span continuous stepped beam, and a three-span continuous non-uniform bridge deck. $m(x)$ shown in Fig. 1 is the mass per unit length of the beam; $E(x)$ and c are Young's modulus and damping of the beam, respectively; $I(x)$ is the moment of inertia for the cross-section of the beam; $y(x, t)$ is the vertical displacement of the beam at position x and time t. The location of the vehicle is defined by the vehicle coordinate s. As a result, $\dot{s}$ and $\ddot{s}$ are the velocity and acceleration of the vehicle, respectively. It was assumed that

the bridge was in equilibrium under its own weight before the presence of the vehicle on the bridge, and the wheels of the vehicle remain in contact with the bridge surface at all times.
The equations of motion of the vehicle are derived as:

$$m_p\ddot{x}_1 + c_p(\dot{x}_1 - \dot{x}_2 - \dot{x}_3 l_3) + k_p(x_1 - x_2 - x_3 l_3) = m_p\ddot{s}y'_p \tag{1}$$

$$\begin{aligned} &m_b\ddot{x}_2 + c_p(\dot{x}_2 + \dot{x}_3 l_3 - \dot{x}_1) + k_p(x_2 + x_3 l_3 - x_1) \\ &\quad + c_r(\dot{x}_2 - \dot{x}_3 l_2 - \dot{x}_5) + k_r(x_2 - x_3 l_2 - x_5) + c_f(\dot{x}_2 + \dot{x}_3 l_1 - \dot{x}_4) \\ &\quad + k_f(x_2 + x_3 l_1 - x_4) = m_b\ddot{s}y'_b \end{aligned} \tag{2}$$

$$\begin{aligned} &J\ddot{x}_3 + c_p(\dot{x}_2 + \dot{x}_3 l_3 - \dot{x}_1) l_3 + k_p(x_2 + x_3 l_3 - x_1) l_3 \\ &\quad + c_r(\dot{x}_3 l_2 + \dot{x}_5 - \dot{x}_2) l_2 + k_r(x_3 l_2 + x_5 - x_2) l_2 \\ &\quad + c_f(\dot{x}_2 + \dot{x}_3 l_1 - \dot{x}_4) l_1 + k_f(x_2 + x_3 l_1 - x_4) l_1 = 0 \end{aligned} \tag{3}$$

$$\begin{aligned} &m_f\ddot{x}_4 + c_f(\dot{x}_4 - \dot{x}_3 l_1 - \dot{x}_2) + k_f(x_4 - x_3 l_1 - x_2) \\ &\quad + k_{tf}(x_4 + y_f) - m_f\ddot{s}y'_f = k_{tf} q_f \end{aligned} \tag{4}$$

$$\begin{aligned} &m_r\ddot{x}_5 + c_r(\dot{x}_5 + \dot{x}_3 l_2 - \dot{x}_2) + k_r(x_5 + x_3 l_2 - x_2) \\ &\quad + k_{tr}(x_5 + y_r) - m_r\ddot{s}y'_r = k_{tr} q_r. \end{aligned} \tag{5}$$

The equation of motion of the beam can be written as:

$$\begin{aligned} &EI(x)y'''' + m(x)\ddot{y} + c\dot{y} = [G_1 - k_{tf} q_f \\ &\quad + k_{tf}(x_4 + y_f)]\delta(x - s - l_1) \\ &\quad + [G_2 - k_{tr} q_r + k_{tr}(x_5 + y_r)]\delta(x - s + l_2) \end{aligned} \tag{6}$$

where y_p, y_b, y_f, and y_r are the displacements of the beam at the location of the centroid of the cab, the tractor, and the front and rear axles, respectively. G_1 and G_2 are the vehicle gravity distributed to the front and rear axles, respectively.

With the modal superposition technique, the displacements of the beam $y(x, t)$ can be expressed as:

$$y(x, t) = \sum_{i=1}^{N} \xi_i(t) \cdot \phi_i(x) \tag{7}$$

where N is the total number of modes used for the beam under consideration; $\xi_i(t)$ and $\phi_i(x)$ are the ith generalized modal coordinate and the ith mode shape of the beam, respectively. Using the modal superposition technique, the Eq. (6) can be written as:

$$\begin{aligned} \ddot{\xi}_i(t) + 2\omega_i\eta_i\dot{\xi}_i(t) + \omega_i^2\xi_i(t) = &\Bigg[G_1 - k_{tf} q_f \\ &+ k_{tf}\left(x_4 + \sum_{i=1}^{m}\xi_i(t)\cdot\phi_i(x)\bigg|_{x=s+l_1}\right)\Bigg]\phi_n(s + l_1) \\ &+ \left[G_2 - k_{tr} q_r + k_{tr}\left(x_5 + \sum_{i=1}^{m}\xi_i(t)\cdot\phi_i(x)\bigg|_{s-l_2}\right)\right]\phi_n(s - l_2) \end{aligned} \tag{8}$$

where ω_i is the natural frequencies of the beam, η_i is the percentage of the critical damping for the ith mode of the beam.
Eqs. (1)–(5) and (8) can be rewritten in the matrix form as:

$$M\ddot{U} + C\dot{U} + KU = P \tag{9}$$

where M, C, and K are the mass, damping, and stiffness matrices of the vehicle–bridge system, respectively; P and U are the global load vector and the global displacement vector of the entire system, respectively, and written as:

$$\begin{aligned} P \;=\; &[0\ 0\ 0\ k_{tf} q_f k_{tr} q_r (G_1 - k_{tf} q_f)\phi_1(s + l_1) \\ &+ (G_2 - k_{tr} q_r)\phi_1(s - l_2) \cdots (G_1 - k_{tf} q_f)\phi_m(s + l_1) \\ &+ (G_2 - k_{tr} q_r)\phi_m(s - l_2)]^T \end{aligned}$$

$$U = \begin{bmatrix} x_1 & x_2 & x_3 & x_4 & x_5 & \xi_1 & \xi_2 \cdots & \xi_m \end{bmatrix}^T.$$

Eq. (9) can then be solved using the Newmark-β method. In the present study, the damping of bridge structures was assumed to be of the Rayleigh type.

3. Simulation of non-stationary random response of the wheels

3.1. Simulation of non-stationary random response of the front wheel

As discussed earlier, a road roughness is usually regarded as a stationary random process in space domain. If a vehicle travels with a constant speed, on account of the relationship between the moving distance (s) and time (t), the road roughness is also a stationary random process in time domain. When study a bridge vibration under moving vehicles with constant speed, this stationary can be used as the inputs. However, the responses of the tires are essentially a non-stationary random process in time domain while a vehicle travels at variable speeds. Nigam and Yaday [34], Hammond and Harrison [38], and Hwang and Kim [35] proposed different methods for solving the non-stationary random process, but the computation efforts required by their method were very large. Therefore, this section presents a new method of obtaining the non-stationary random response by using the covariance equivalence technique.

The Power Spectral Density (PSD) of road roughness in space domain can be expressed as:

$$s_q(n) = s_q(n_0)n_0^2/n^2, \tag{10}$$

where $s_q(n)$ is the spatial power spectral density; $s_q(n_0)$ is called the coefficient of road roughness; n is spatial frequency (1 /m); and $n_0 = 1/2\pi$. The relationship between the spatial angular frequency and spatial frequency can be expressed as $\Omega_q = 2\pi n$, and Eq. (10) can be rewritten as

$$s_q(\Omega_q) = s_q(n_0)n_0^2/\Omega_q^2. \tag{11}$$

In Eq. (11), when $\Omega_q \to 0$, $s_q(\Omega_q) \to \infty$; an improved equation for the PSD of road roughness in frequency domain is introduced as

$$s_q(\Omega_q) = s_q(n_0)n_0^2/(\Omega_q^2 + \Omega_c^2), \tag{12}$$

where $\Omega_c = 2\pi n_c$ is the lowest cut-off angular frequency.

Eq. (12) can be considered as a response of a first order linear system to white noise excitations. Based on the theory of random vibration, the following relationship can be obtained from [36].

$$s_q(\Omega_q) = \left|H(\Omega_q)\right|^2 S_W, \tag{13}$$

where $H(\Omega_q)$ is the transfer function; and S_W is the PSD of white noise and it is normally equal to 1. Based on Eq. (11), $H(\Omega)$ can be written as:

$$H(\Omega) = \frac{n_0\sqrt{s_q(n_0)}}{\Omega_c + j\Omega}. \tag{14}$$

From Eq. (14), the differential equation of road roughness can be expressed as:

$$\frac{\mathrm{d}q_f(s_c)}{\mathrm{d}s_c} + \Omega_c q_f(s_c) = n_0\sqrt{s_q(n_0)}W(s_c), \tag{15}$$

where $W(s_c)$ is the stationary white noise processes in space domain, $q_f(s_c)$ is the stationary random response in space domain, and s_c is the position of the front wheel from the entrance of the bridge.

In order to derive the response in time domain, the following equation needs to be introduced:

$$\frac{\mathrm{d}q_f(s_c)}{\mathrm{d}s_c} = \frac{1}{\dot{s}_c}\frac{\mathrm{d}q_f(t)}{\mathrm{d}t}, \tag{16}$$

where $q_f(t)$ is a non-stationary random response induced by the road roughness in time domain, when the vehicle travels with a variable speed $\dot{s}_c$, which is a function of time t.

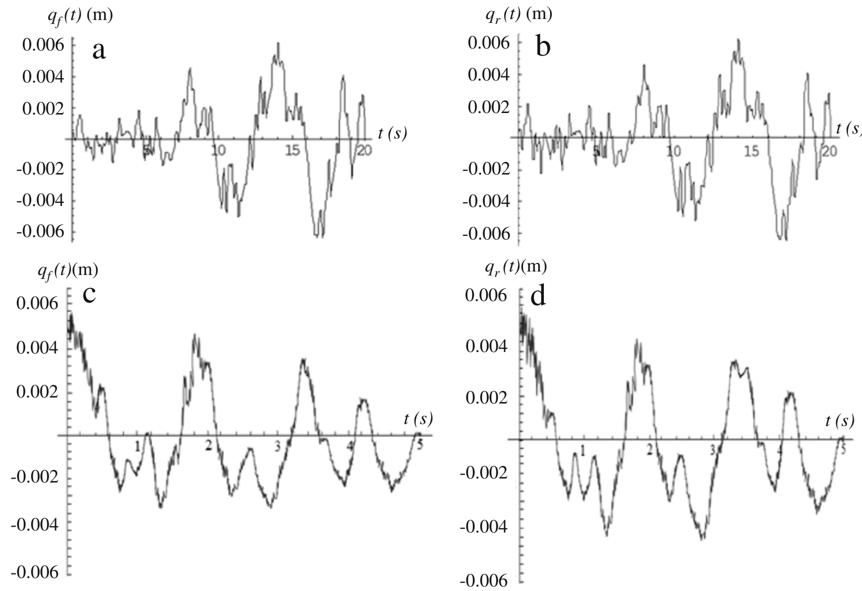

Fig. 2. Samples of time history of non-stationary random responses with vehicle moving at variable speed:(a) front wheel response with vehicle moving at $\dot{s} = 0$ (m/s); $\ddot{s} = 2$ (m/s^2); (b) rear wheel response with vehicle moving at $\dot{s} = 0$ (m/s); $\ddot{s} = 2$ (m/s^2); (c) front wheel response with vehicle moving at $\dot{s} = 20$ (m/s); $\ddot{s} = -4$ (m/s^2); (d) rear wheel response with vehicle moving at $\dot{s} = 20$ (m/s); $\ddot{s} = -4$ (m/s^2).

Substituting Eq. (16) into Eq. (15), the following can be obtained:

$$\dot{q}_f(t) + \dot{s}_c \Omega_c q_f(t) = n_0 \dot{s}_c \sqrt{s_q(n_0)} W[s_c(t)]. \tag{17}$$

$W[s_c(t)]$ is a non-stationary white noise processes having a frequency modulated form in time domain, the technique of the evolutionary spectral analysis cannot be directly used. To solve the Eq. (17), it is necessary to transfer the non-stationary white noise processes into the stationary white noise processes. The technique of covariance equivalence is one of the effective methods to transfer the non-stationary white noise processes into the stationary white noise processes. The main focus of this technique is introducing a stationary white noise process, whose covariance equals to the covariance of the non-stationary white noise process. The details of the technique of covariance equivalence can be obtained from [36,39].

By introducing stationary white noise process $W_1(t)$ instead of non-stationary white noise process $W[s_c(t)]$, and using the technique of covariance equivalence [36,39],

$$E\{W[s_c(t_1)]W[s_c(t_2)]\} = \delta[s_c(t_2) - s_c(t_1)] = \frac{\delta(t_2 - t_1)}{\dot{s}_c(t_1)} \tag{18}$$

and

$$E\left[\frac{W_1(t_1)}{\sqrt{\dot{s}_c(t_1)}} \frac{W_1(t_2)}{\sqrt{\dot{s}_c(t_2)}}\right] = \frac{\delta(t_2 - t_1)}{\dot{s}_c(t_1)}, \tag{19}$$

where $W_1(t)$ is the stationary white noise process, $\delta(\cdot)$ is the Dirac delta function, and comparing Eqs. (18) and (19), it can be found that the covariant of $W[s_c(t)]$ and $\frac{W_1(t)}{\sqrt{\dot{s}_c}}$ are equivalent. Hence Eq. (17) becomes as

$$\dot{q}_f(t) + \dot{s}_c \Omega_c q_f(t) = n_0 \sqrt{s_q(n_0) \dot{s}_c} W_1(t), \tag{20}$$

Eq. (20) is the equation of obtaining the non-stationary random response induced by the road roughness of front wheel.

3.2. Simulation of non-stationary random response of the rear wheel

The description of correlated disturbances between front and rear wheels can be written as follows:

$$q_r(t) = q_f[t - \tau] \tag{21}$$

where $q_r(t)$ is the non-stationary random response of the rear wheel in time domain; $q_f(t)$ is the non-stationary random response of the front wheel in time domain; τ is the interval time between the front and rear wheels.
Due to the τ is not the constant for the vehicle moving with varying speed, Eq. (21) cannot be easily used to obtain the non-stationary response of the rear wheel by the method of Fourier transform.
Based on the Ref. [36], the Eq. (21) can be written as:

$$q_r(t) = q_f[s_c(t) - l_c], \tag{22}$$

l_c is the distance between the front and rear wheels and it can be expressed as $l_c = l_1 + l_2$.

By expanding Eq. (22) by the method of Taylor formula and calculating the derivatives and introducing the following expression

$$\frac{\mathrm{d}^2 q_f(s_c)}{\mathrm{d}s_c^2} = \frac{1}{\dot{s}_c^2} \frac{\mathrm{d}^2 q_f(t)}{\mathrm{d}t^2} - \frac{\ddot{s}_c}{\dot{s}_c^3} \frac{\mathrm{d}q_f(t)}{\mathrm{d}t}. \tag{23}$$

The following equation can be obtained

$$\dot{q}_r(t) = (-2\dot{s}_c/l_c) q_r(t) - \dot{q}_f(t) + (2\dot{s}_c/l_c) q_f(t). \tag{24}$$

Eq. (24) is the equation of the non-stationary random response of the rear wheels. To solve the Eqs. (20) and (24), the non-stationary random response of the front and rear wheels can be obtained.

3.3. Comparison of non-stationary and stationary response of the wheels

To compare the difference of non-stationary random response and stationary response to the wheels of the vehicle, two kinds of time history of the responses were generated and were shown in Figs. 2 and 3, respectively. The simulated parameters were as follows: the coefficient of road roughness obtained from the

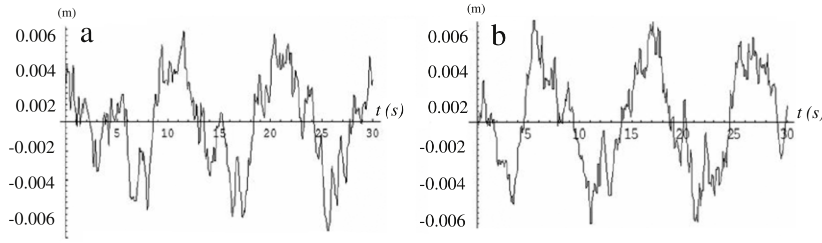

Fig. 3. Samples of time history of stationary random responses: (a) vehicle moving at 5 m/s; (b) vehicle moving at 10 m/s.

Table 1
Classification of road surface roughness.

Description	$s_q(n_0)10^{-6}$ (m^3/cycle)
Good	16
Average	64
Poor	256
Very Poor	1024

International Organization for Standardization [40] was $s_q(n_0) = 64 \times 10^{-6}$ (m^3/cycles); the vehicle started running when initial speed was $\dot{s} = 0$ (m/s) and acceleration was $\ddot{s} = 2$ (m/s^2). Using Eqs. (20) and (24) for non-stationary random responses, Fig. 2(a) and (b) show the amplitude of wheel's responses $q_f(t)$ and $q_r(t)$ produced by road roughness increases as the time goes due to the increases of vehicle velocity. While the vehicle moving with deceleration, Fig. 2(c) and (d) show the amplitude of wheel's responses decreases as the time goes due to the decreases of velocity. As vehicular speed approaches to zero, so does the effective $q_f(t)$ and $q_r(t)$. If the vehicle moves with a constant speed, two samples of time history of stationary random responses for 5 m/s and 10 m/s were obtained like the Refs. [24–26] and also shown in Fig. 3, which shows the amplitude of wheel's response is stationary, and the vehicle velocity almost has no effect on the amplitude of wheel's response. Figs. 2 and 3 show obvious difference between stationary random responses and non-stationary random response for the vehicle wheels. It is very clear that the vibration of the vehicle with acceleration is more severe than the vibration of the vehicle with constant velocity. This can be explained very well from the samples of non-stationary random responses. Therefore, the simulation of non-stationary random responses to tires is more accurate than the simulation in other papers.

4. Numerical study

The 5-DOF vehicle model shown in Fig. 1 was used in the numerical study. The parameters of the vehicle, introduced in precious sections, were directly taken from another study [41], and are shown as follows:

$$m_p = 850 \text{ kg}; \quad m_b = 21.015 \times 10^3 \text{ kg}; \quad m_r = m_f = 2500 \text{ kg};$$
$$l_1 = 1.2 \text{ m}; \quad l_2 = 3 \text{ m};$$
$$k_p = 230\,710 \text{ N/m}; \quad k_r = 2029\,200 \text{ N/m};$$
$$k_f = 1932\,600 \text{ N/m}; \quad k_{tr} = 3700\,000 \text{ N/m};$$
$$k_{tf} = 2080\,000 \text{ N/m};$$
$$c_p = 15\,000 \text{ N s/m}; \quad c_f = c_r = 10\,000 \text{ N s/m}.$$

The road surface roughness used in the present study was based on the Ref. [40]. The values of $s_q(n_0)$ used in the present study are given in Table 1.

The dynamic impact factor of the bridge subjected to moving vehicle loading is calculated as:

$$I = R_{dm}/R_{sm} - 1 \tag{25}$$

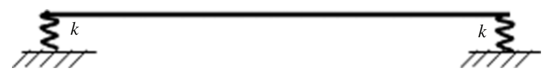

Fig. 4. The model of the bridge.

where R_{dm} and R_{sm} denote the maximum vertical dynamic and static deflections of the bridge under the vehicle loading, respectively.

When the vehicle travels at variable speed, the stationary random process like the Refs. [24–26] and the non-stationary response of tires, in time domain, were considered, and they were both used as inputs in the bridge–vehicle coupled system. The effects of the two different inputs on the impact factor were then compared as follows.

4.1. Example 1: a uniform single-span bridge deck supported by elastomeric bearings

In bridge design, elastic bearings are usually installed between the bridge girders and the cap beam of the supporting structure to reduce the vibration of the superstructure. The dynamic response of bridge deck supported by elastomeric bearings subjected to moving loads was analyzed by Yau et al. [42] and Chen et al. [43]. Therefore, the model of the bridge deck supported by elastomeric bearings is typical. In the present study, the model of the bridge deck used by Chen et al. [43], as shown in Fig. 4, was used. The parameters of the bridge deck used are as follows:

$$m = 1.5 \times 10^4 \text{ kg/m}, \quad E = 2 \times 10^{11} \text{ N/m}^2,$$
$$I = 0.048 \text{ m}^4, \quad l = 30 \text{ m}, \quad k,$$

where m is the mass per unit length of the bridge deck; E is the Young's modulus of the bridge deck; k is the elastomeric bearing and is calculated in obtaining the mode shape of the beam; and l is the length of the bridge deck. In the reference studied by [43], the stationary responses of the beam under vehicular load with constant speed were obtained. To verify the accuracy of the present computational program, it should be the best way to compare with the non-stationary responses of the beam obtained by other researchers. However, to the best of the writers' knowledge, few references for the studying the non-stationary responses of a beam under vehicular loads are available. The present computational program also can study the stationary responses under vehicular loads when the vehicles moving with constant speeds. Therefore, the deflection of the beam at mid-span obtained in the present study was compared to that obtained by [43]. The first three modes of the beam were used for the solution of the equations, and the time-step in Newmark-β method was taken as 0.005 s. Fig. 5 shows the comparison of the effects of vehicular speed on the mid-span deflections in this study and those from [43] with two different elastomeric bearings. One can find that the results obtained in this study match the results from [43] very well.

The effects of the two random inputs on the impact factors were studied in the following using different parameters for the

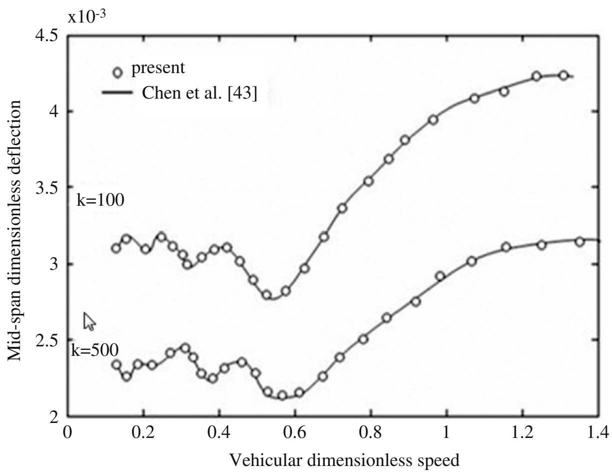

Fig. 5. Comparison of mid-span deflections of the present study and those from [43].

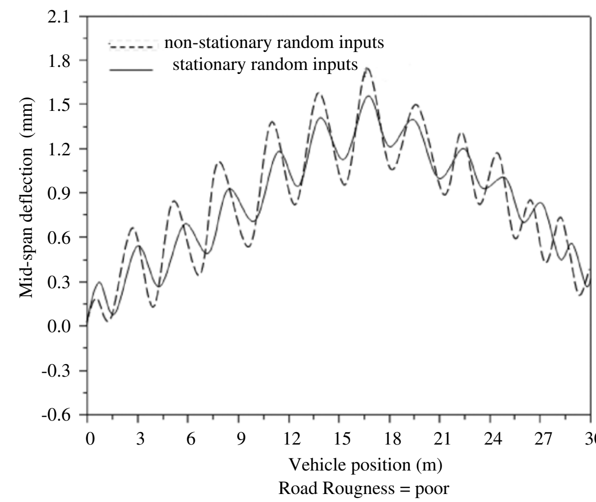

Fig. 7. The mid-span deflections of the beam versus vehicle positions.

vehicle–bridge system. Three common initial speeds, 5 m/s, 10 m/s, and 15 m/s, for vehicle were used, and two acceleration, 4 m/s^2 and 6 m/s^2, were considered. Two different coefficients of road surface roughness, $s_q(n_0) = 64 \times 10^{-6}$ (m^3/cycle) for Average and $s_q(n_0) = 256 \times 10^{-6}$ (m^3/cycle) for Poor, were considered.

Fig. 6 shows the effect of the two different kinds of inputs on the mid-span deflection of the beam when the vehicle moving with $\dot{s} = 10$ m/s; $\ddot{s} = 4$ m/s^2. Fig. 6(a) shows that the impact factors are $I = 0.127$ and $I = 0.212$ for the stationary and non-stationary random inputs, respectively. Fig. 6(b) shows that the impact factors resulted from the stationary and non-stationary random inputs are $I = 0.213$ and $I = 0.323$, respectively. In both cases, the difference between stationary and non-stationary inputs is significant.

To compare the solutions of the two different random inputs on the impact factors with different accelerations when the other parameters remain the same, the solutions with vehicular speed $\dot{s} = 10$ m/s; $\ddot{s} = 6$ m/s^2 are computed and shown in Fig. 7. Comparing the mid-span deflections from Fig. 6(a) with those in Fig. 7, it can be seen that when the acceleration varies, the mid-span deflections are also affected by the two different kinds of model of random inputs. For example, for the model of non-stationary random inputs, the maximum mid-span deflections are 1.53 (mm) and 1.73 (mm) for $\ddot{s} = 4$ m/s^2 and $\ddot{s} = 6$ m/s^2, respectively.

More cases with different combination of parameters including the coefficients of road surface, initial speeds, and accelerations were investigated and results are summarized in Tables 2–4.

The results indicate that different simulations of the random inputs can lead to different mid-span deflections and impact factors; these differences can be easily explained from the simulation of the responses induced by road surface of the wheels discussed earlier. Therefore, for single-span bridge deck supported by elastomeric bearing, a proper random model simulating the road surface to vehicle with variable speed is an important factor in the impact factors studies.

Since structural dynamic performance of bridges depends on parameters like stiffness, damping and boundary condition etc. it is necessary to study the effects of stationary and non-stationary random inputs on different bridge types. This paper mainly focuses on the beam bridge types, the other bridge types will be studied in a future paper. To study the dynamic performance of different beam bridge types, two typical beam bridge models were introduced by Zhu and Law [2] and Dugush and Eisenberger [44]: a three-span stepped beam with equal spans and a three-span continuous non-uniform bridge deck. For this reason, those two bridge models were also studied and will be discussed next.

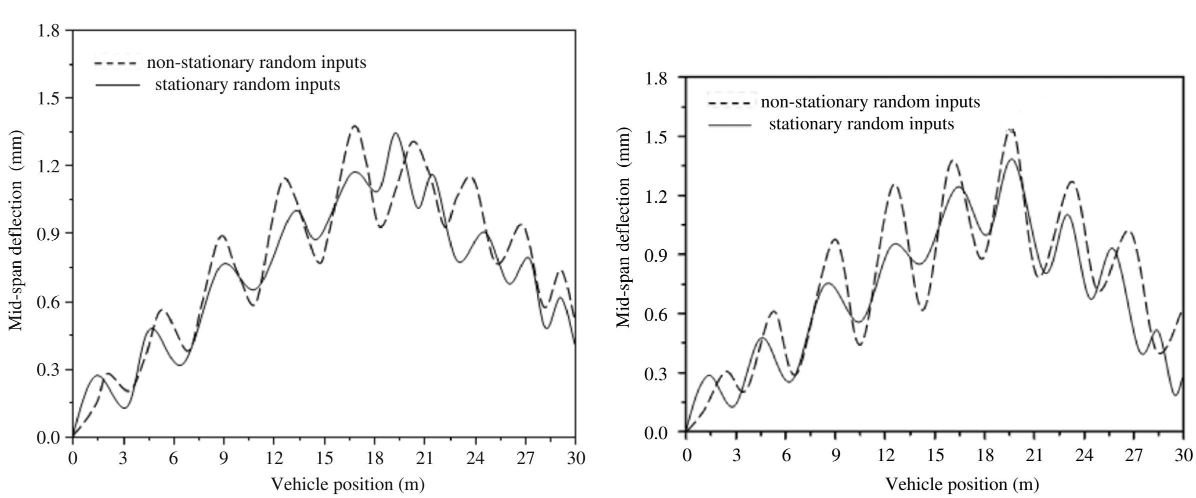

(a) Road roughness = Average. (b) Road roughness = Poor.

Fig. 6. Effect of different type of random inputs on the mid-span deflection of the beam under different coefficients of road surface: (a) Road roughness = Average (b) Road roughness = Poor.

Table 2
Comparison of impact factors under the two different random inputs with good road surface roughness $s_q(n_0) = 16 \times 10^{-6}$ (m^3/cycle).

Coefficients of road surface roughness		$s_q(n_0) = 16 \times 10^{-6}$ (m^3/cycle)								
Initial speed (m/s)		5			10			15		
Acceleration (m/s^2)		2	4	6	2	4	6	2	4	6
Impact factors	Stationary random inputs	0.053	0.084	0.173	0.086	0.104	0.213	0.107	0.227	0.257
	Non-stationary random inputs	0.067	0.105	0.188	0.109	0.123	0.243	0.225	0.248	0.336

Table 3
Comparison of impact factors under the two different random inputs with average road surface roughness $s_q(n_0) = 64 \times 10^{-6}$ (m^3/cycle).

Coefficients of road surface roughness		$s_q(n_0) = 64 \times 10^{-6}$ (m^3/cycle)								
Initial speed (m/s)		5			10			15		
Acceleration (m/s^2)		2	4	6	2	4	6	2	4	6
Impact factors	Stationary random inputs	0.061	0.102	0.165	0.105	0.127	0.195	0.138	0.233	0.274
	Non-stationary random inputs	0.072	0.123	0.184	0.127	0.212	0.246	0.231	0.266	0.349

Table 4
Comparison of impact factors under the two different random inputs with poor road surface roughness $s_q(n_0) = 256 \times 10^{-6}$ (m^3/cycle).

Coefficients of road surface roughness		$s_q(n_0) = 256 \times 10^{-6}$ (m^3/cycle)								
Initial speed (m/s)		5			10			15		
Acceleration (m/s^2)		2	4	6	2	4	6	2	4	6
Impact factors	Stationary random inputs	0.079	0.113	0.187	0.145	0.177	0.215	0.228	0.245	0.303
	Non-stationary random inputs	0.086	0.134	0.215	0.163	0.234	0.287	0.243	0.290	0.398

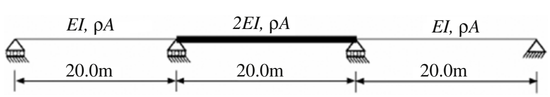

Fig. 8. A three-span stepped beam with equal spans.

4.2. Example 2: a three-span stepped beam with equal spans

The second example shown in Fig. 8 is a three-span beam with uniform sections at each span. The flexural stiffness of the central span is twice that of the side span. Each span length is 20.0 m, and the density per unit length for all beams is assumed to be $\rho A = 1000$ kg/m. The flexural stiffness of the side span is $EI = 1.96 \times 10^6$ kN m^2, and the mode shape function for the beam can be obtained from [44]. The solution of this problem was obtained using the first four mode shapes, and the natural frequencies corresponding to these mode shapes are 38.9, 47.6, 75.3, and 152.1 (rad/s), respectively. When the coefficient of road surface roughness is $s_q(n_0) = 256 \times 10^{-6}$ (m^3/cycle) and vehicular speed is $\dot{s} = 10$ m/s, $\ddot{s} = 4$ m/s^2, the dynamic deflections at mid-span locations of the first and second span are shown in Fig. 9. The effect of vehicular speeds on the impact factors of the central span is shown in Fig. 10. It can be seen that the mid-span deflections and impact factors of the three-span beams are also affected by the two different random inputs. For example, for the model of stationary and non-stationary random inputs shown in Fig. 9(a), the maximum mid-span deflections are 0.96 (mm) and 1.25 (mm), respectively.

The results from this example indicate that different simulations of the random inputs lead to different mid-span deflections and impact factors for both first and central spans. Therefore, for the three-span stepped beam with equal spans, the random models of the road surface inputs is a key factor to the vibration of the vehicle–bridge system.

4.3. Example 3: a three-span continuous non-uniform bridge deck

The bridge deck in example 3 is a three-span continuous non-uniform bridge deck as shown in Fig. 11. The modulus of elasticity of the bridge is $E = 3 \times 10^{10}$ N/m^2 and the density is $\rho =$

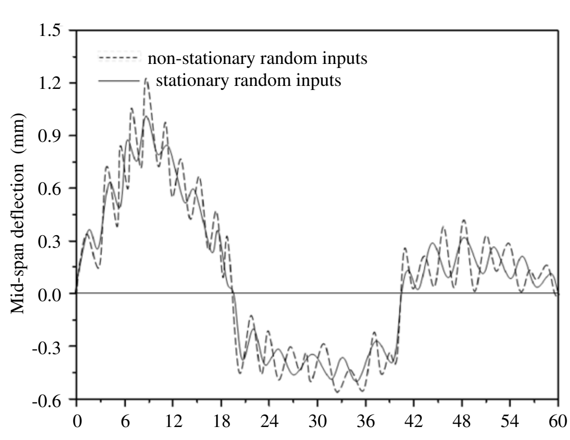

(a) Deflections of the first span.

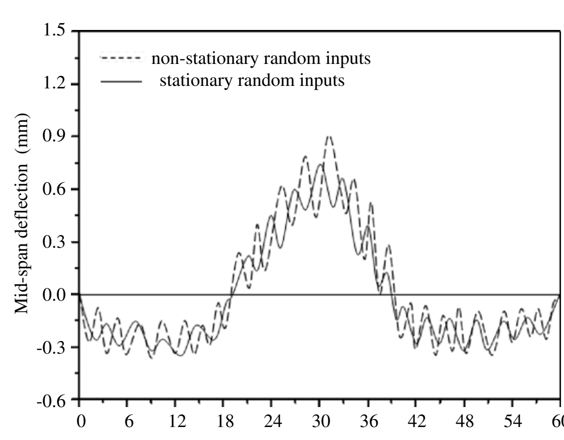

(b) Deflections of the central span.

Fig. 9. Deflections at mid-span positions of (a) the first span and (b) central span.

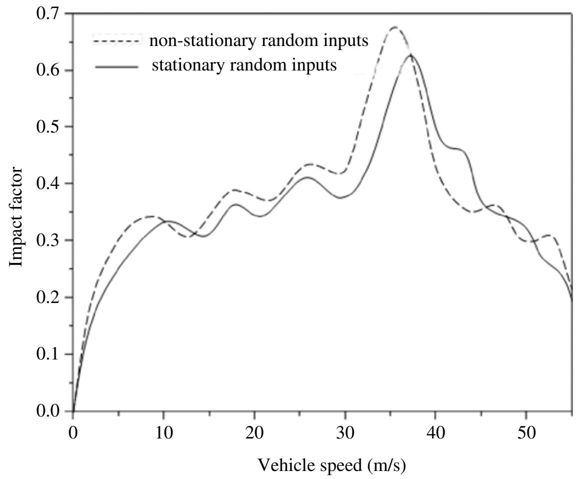

Fig. 10. Impact factor of central span versus vehicular speed.

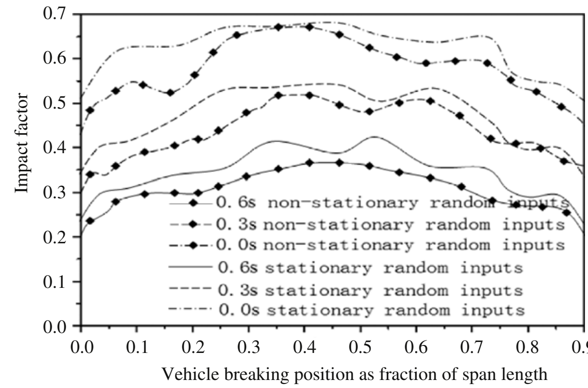

Fig. 12. Impact factors versus different vehicle braking position.

2400 kg/m^3. When studying the effects of the two different models of road surface inputs on the vehicle–bridge system with variable vehicular speeds, the braking is one of the important sources of variable speeds. Yang and Wu [45], Law and Zhu [27], and Ju and Lin [28] all discussed the effect of braking on the dynamic response of bridges. They all concluded that vehicle braking may contribute significantly to bridge response, and that the resulting impact factors may exceed those adopted in current design codes. Therefore, in this example, the effects of the two inputs on the impact factors under the vehicle braking situation were studied. When the vehicular initial speed is $\dot{s} = 10$ m/s, the impact factors were studied with variations of the following parameters obtained from [27]:

(a) braking rise time 0.6, 0.3, 0.0 s;
(b) braking position of the vehicle; and
(c) different road surface roughness as specified in the Ref. [40]. Road surface roughness ranging from Good to Very Poor were used in this study.

Fig. 12 plots the impact factors at the mid-span of the central span against vehicle braking positions when a coefficient of road surface roughness of $s_q(n_0) = 256 \times 10^{-6}$ (m^3/cycle) was used; when the vehicular initial speed is $\dot{s} = 10$ m/s, three different braking rest times 0.6 s, 0.3 s and 0.0 s, and two different random input models, i.e., stationary and non-stationary inputs were used. It shows that the duration of braking rise time and vehicle braking position have very significant effects on the maximum impact factors. For example, the impact factors produced from a braking time 0.6 s is approximately 0.347 while that from sharp braking with 0.0 s is approximately 0.668 for non-stationary random inputs when vehicle brakes at the position of 2/5L.

Table 5 shows the impact factors for different road surface conditions when a vehicle brakes at position 2/5L with a rise time of 0.3 s under three different vehicular initial speeds: $\dot{s} = 5$ m/s, $\dot{s} = 10$ m/s, and $\dot{s} = 15$ m/s. It can be observed that the effect of the two different inputs on the impact factors is significant. Using the stationary random process inputs to model the road surface disturbance to vehicles with variable speed will lead to underestimating impact factors in some cases and overestimating them in the other cases. This is different from the cases of acceleration (see Tables 2–4) where stationary inputs always underestimate the impact factors.

5. Conclusions

This paper presented a new method for analyzing the non-stationary random response of bridges. Using the covariance equivalence technique, the time domain non-stationary random responses of the vehicles wheels with variable speed were obtained. A two-axle vehicle model was used. Three typical bridge models were analyzed: a single-span uniform Bernoulli–Euler beam, a three-span stepped beam and a three-span continuous non-uniform bridge deck. The differential equations of motion of coupled systems were derived. The stationary random process and

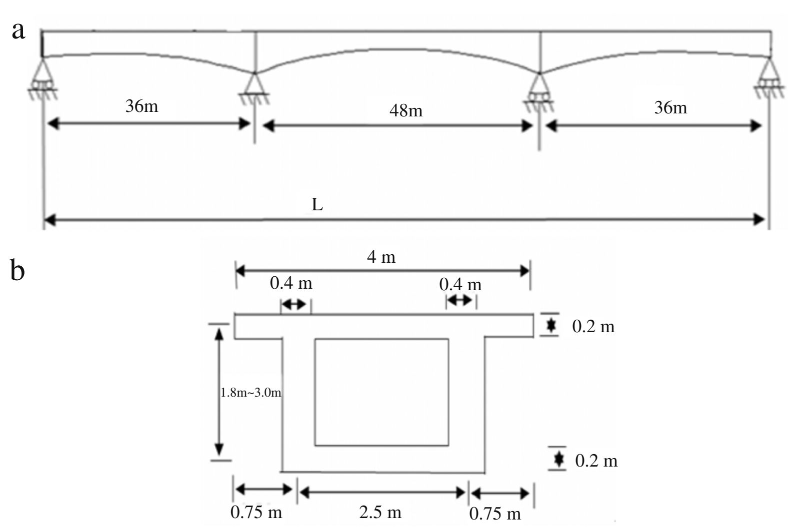

Fig. 11. A three-span continuous non-uniform bridge deck.

Table 5
Impact factors with different road surface conditions.

Road class		Good	Average	Poor	Very Poor
$\dot{s} = 5$ m/s	Non-stationary random inputs	0.068	0.187	0.356	0.558
	Stationary random inputs	0.073	0.189	0.412	0.601
$\dot{s} = 10$ m/s	Non-stationary random inputs	0.158	0.267	0.518	0.684
	Stationary random inputs	0.167	0.286	0.547	0.723
$\dot{s} = 15$ m/s	Non-stationary random inputs	0.298	0.397	0.656	0.989
	Stationary random inputs	0.330	0.441	0.766	1.219

the non-stationary response of tires are respectively treated as the inputs of the bridge–vehicle coupled system. The comparison of the effect of the two inputs on the mid-span deflection and the impact factors were compared with different parameters including the coefficient of surface roughness, vehicle acceleration, and vehicle braking. Numerical results indicate that: (1) the amplitude of non-stationary random responses of the wheels increases as the vehicle velocity increases, and decreases with the decreases in vehicle velocity; (2) if taking the stationary random process to model the road surface disturbance to vehicle with variable speed, it may either underestimate or overestimate the dynamic effects; (3) factors such as different road surface roughness coefficients, initial vehicular speeds, vehicle accelerations, and vehicle braking conditions have very significant influence on the impact factors under both stationary and non-stationary random inputs.

References

[1] Henchi K, Fafard M, Talbot M, Dhatt G. An efficient algorithm for dynamic analysis of bridges under moving vehicles using a coupled modal and physical components approach. J Sound Vibration 1998;212(4):663–83.
[2] Zhu XQ, Law SS. Moving forces identification on a multi-span continuous bridge. J Sound Vibration 1999;228(2):377–96.
[3] Law SS, Bu JQ, Zhu XQ. Vehicle axle loads identification using finite element method. Eng Struct 2004;26(8):1143–53.
[4] Silva D. Dynamical performance of highway bridge decks with irregular pavement surface. Comput Struct 2004;82(11):871–81.
[5] Wang TL, Huang DZ, Shahawy M. Dynamic response of multi-girder bridges. J Struct Eng 1992;118(8):2222–38.
[6] Liu CH, Huang DZ, Wang TL. Analytical dynamic impact study based on correlated road roughness. Comput Struct 2002;80(20):1639–50.
[7] Chatterjee PK, Datta TK, Surana CS. Vibration of continuous bridges under moving vehicles. J Sound Vibration 1994;169(5):619–32.
[8] Green MF, Cebon D. Dynamic interaction between heavy vehicles and highway bridges. Comput Struct 1997;62(2):253–64.
[9] Lu S, Deng XJ. Prediction vertical dynamic loads caused by vehicle–pavement interaction. J Transp Eng 1998;124(5):470–7.
[10] Chen SR, Cai CS. Accident assessment of vehicles on long-span bridges in windy environments. J Wind Eng Ind Aerodyn 2004;92(12):991–1024.
[11] Zhang Y, Cai CS, Shi XM. Vehicle induced dynamic performance of a FRP versus concrete slab bridge. ASCE J Bridge Eng 2006;11(4):410–9.
[12] Zheng Y, Das PK. Improved response surface method and its application to stiffened plate reliability analysis. Eng Struct 2000;22(5):544–51.
[13] Pinkaew T, Asnachinda P. Experimental study on the identification of dynamic axle loads of moving vehicles from the bending moments of bridges. Eng Struct 2007;29(10):2282–93.
[14] Cheng J, Zhang J, Cai CS, Xiao RC. A new approach for solving inverse reliability problems with implicit response functions. Eng Struct 2007;29(1):71–9.
[15] Cai CS, Shi XM, Araujo M, Chen S. Effect of approach span condition on vehicle-induced dynamic response of slab-on-girder road bridges. Eng Struct 2007;29(12):3210–26.
[16] Dinh VN, Kim KD, Warnitchai P. Dynamic analysis of three-dimensional bridge-high-speed train interactions using a wheel–rail contact model. Eng Struct 2009;31(12):3090–106.
[17] Ronagh HR, Moghimi H. Development of a numerical model for bridge–vehicle interaction and human response to traffic-induced vibration. Eng Struct 2008;30(12):3808–19.
[18] Yang YB, Lin BH. Vehicle-bridge interaction analysis by dynamic condensation method. J Struct Eng 1995;121(11):1636–43.
[19] Yang F, Fonder GA. An iterative solution method for dynamic response of bridge–vehicles systems. Earthq Eng Struct Dyn 1996;25(2):195–215.
[20] Fryba L. Response of a beam to a rolling mass in the presence of adhesion. Acta Tech CSAV 1974;19(6):673–87.
[21] Gupta RK, Traill-Nash RW. Vehicle braking on highway bridges. J Eng Mech Div 1980;106(4):641–58.
[22] Mulcahy NL. Bridge response with tractor-trailer vehicle loading. Earthq Eng Struct Dyn 1983;11(5):649–65.
[23] Chompooming K, Yener M. The influence of roadway surface irregularities and vehicle deceleration on bridge dynamics using the method of lines. J Sound Vibration 1995;183(4):567–89.
[24] Toth J, Ruge P. Spectral assessment of mesh adaptations for the analysis of the dynamical longitudinal behavior of railway bridges. Arch Appl Mech 2001;71(7):453–62.
[25] Berghuvud A. Freight car curving performance in braked conditions. Proc Inst Mech Eng Part F. J Rail Rapid Transit 2002;216(1):23–9.
[26] Hu HY, Han Q. Three dimensional modeling and dynamic analysis of four-wheel-steering vehicles. Acta Mech Sin 2003;19(1):79–88.
[27] Law SS, Zhu XQ. Bridge dynamic responses due to road surface roughness and braking of vehicle. J Sound Vibration 2005;282(5):805–30.
[28] Ju SH, Lin HT. A finite element model of vehicle–bridge interaction considering braking and acceleration. J Sound Vibration 2007;303(1):46–57.
[29] Honda H, Kajkawa Y, Kobori T. Spectra of road surfaces in bridges. J Struct Eng ASCE 1982;108(8):1956–66.
[30] Dodds CJ, Robson JD. The description of road surface roughness. J Sound Vibration 1983;31(2):175–83.
[31] Marcondes J, Burgess GJ, Harichandran R, Snyder MB. Spectral analysis of highway pavement roughness. J Transp Eng ASCE 1991;117(5):540–9.
[32] Virchis VJ, Robson JD. Response of an accelerating vehicle to random road undulations. J Sound Vibration 1971;18(3):423–71.
[33] Hammond JK, Harrison RF. Non-stationary response of vehicles on rough ground. J Dyn Syst, Meas Control Trans ASME 1981;103(3):245–50.
[34] Nigam NC, Yadav D. Dynamic response of accelerating vehicles to ground roughness, In: Proc. noise shock and vibration conference. Monash University. 1974. p. 280–5.
[35] Hwang JH, Kim JS. On the approximate solution aircraft landing gear under non-stationary random excitations. KSME Int J 2000;14(9):968–77.
[36] Zhang LJ, Lee CM, Wang YS. A study on non-stationary random vibration of a vehicle in time and frequency domains. J Automot Tech 2002;3(3):101–9.
[37] Sasidhar MN, Talukdar S. Non-stationary response of bridge due to eccentrically moving vehicles at non-uniform velocity. J Adv Struct Eng 2003;6(4):309–24.
[38] Hammond JK, Harrison RF. Non-stationary response of vehicle on rough ground—a state space approach. J Dyn Syst Meas Control Trans ASME 1981;103(3):245–50.
[39] Lee JS, Hammond JK. Estimation of parameters of a non-stationary random process due to a moving source based on the covariance-equivalent model. Mech Syst Signal Process 1995;9(5):509–14.
[40] ISO/TC108/WG9 Road surface profiles—reporting of measured data. 1972.
[41] Crolla D, Yu F. Vehicle dynamics and control[M]. Beijing China Communication Press; 2004 [in Chinese].
[42] Yau JD, Wu YS, Yang YB. Impact response of bridges with elastic bearings to moving loads. J Sound Vibration 2001;248(1):8–30.
[43] Chen YH, Tan CA, Bergman LA. Effects of boundary flexibility on the vibration of a continuum with a moving oscillator. Trans ASME. J Vib Acoust 2002;124(4):552–60.
[44] Dugush YA, Eisenberger M. Vibration of non-uniform continuous beams under moving loads. J Sound Vibration 2002;254(5):911–26.
[45] Yang YB, Wu YS. A versatile element for analyzing vehicle–bridge interaction response. Eng Struct 2001;23(5):452–69.